



ORIGINAL ARTICLE

# Zinc oxide nanoparticle synthesized from *Euphorbia fischeriana* root inhibits the cancer cell growth through modulation of apoptotic signaling pathways in lung cancer cells

Haitao Zhang<sup>a,1</sup>, Zhen Liang<sup>b,1</sup>, Jipeng Zhang<sup>d</sup>, Wu-ping Wang<sup>d</sup>, Hui Zhang<sup>c,1,\*</sup>, Qiang Lu<sup>d,1,\*</sup>

<sup>a</sup> Department of Respiratory and Critical Care Medicine, Tangdu Hospital, Air Force Military Medical University, Shanxi, Xi'an 710038, China

<sup>b</sup> First Department of Thoracic Surgery, Peking University Cancer Hospital & Institute, Beijing Institute for Cancer Research, Key Laboratory of Carcinogenesis and Translational Research, China

<sup>c</sup> Department of Traditional Chinese Medicine, The Second Affiliated Hospital of Air Force Medical University, Shanxi, Xi'an 710038, China

<sup>d</sup> Department of Thoracic Surgery, Tangdu Hospital, Air Force Medical University, Shanxi, Xi'an 710038, China

Received 16 March 2020; accepted 16 May 2020

Available online 22 May 2020

## KEYWORDS

Zinc oxide nanoparticle;  
*Euphorbia fischeriana*;  
Lung cancer;  
Apoptosis;  
A549 cells

**Abstract** Lung cancer is the widespread carcinogenesis in men and the third most familiar cancer in women. It is one of the mostly aggressive human cancers, which is responsible for around 1.4 million deaths per annum and has utmost mortality and incidence with 1.8 million new incidences and 1.6 million new deaths yearly. In this present study, we have evaluated the anticancer potential of zinc oxide nanoparticles (ZnONPs) synthesized from a root extract of *Euphorbia fischeriana* (EF), through the apoptosis signaling markers in A549 lung cancer cells. The synthesized EF-ZnONPs were evaluated through the transmission electron microscope (TEM), Fourier transform infra red (FTIR), UV-visible spectroscopy and dynamic light scattering (DLS) techniques. The EF-ZnONPs were assessed for their cytotoxicity activity towards A549 cells by MTT test. The induction of apoptosis was analysed by the mitochondria membrane potential (MMP), reactive oxygen

\* Corresponding authors at: Department of Thoracic Surgery, Tangdu Hospital, Air Force Medical University, Shanxi, Xi'an 710038, China.

E-mail address: [luqiang@fmmu.edu.cn](mailto:luqiang@fmmu.edu.cn) (Q. Lu).

<sup>1</sup> Equal contribution.

Peer review under responsibility of King Saud University.



Production and hosting by Elsevier

species (ROS), cell migration and dual staining. Furthermore, pro and anti-apoptotic signaling protein expression was evaluated by western blotting method. We found the bioformulated EF-ZnONPs has a spherical morphology and revealed the existence of diverse bioactive compounds. Also we found the cytotoxic effect of EF-ZnONPs. Apoptosis was activated by the EF-ZnONPs with improved ROS, decreased MMP, inhibited cell migration and altered dual staining was observed. Furthermore, the diminished expression of anti-apoptotic protein Bcl-2 was noted. In this study, we observed the formulation, characterization and anticancer potency of ZnONPs of EF plant extract (EF-ZnONPs) was useful for treatments of lung cancer.

© 2020 The Author(s). Published by Elsevier B.V. on behalf of King Saud University. This is an open access article under the CC BY-NC-ND license (<http://creativecommons.org/licenses/by-nc-nd/4.0/>).

## 1. Introduction

Cancer is a prime cause of morbidity and mortality about the globe and the quantity of cases are frequently rising predictable to be 21 million by 2030 (Ismail et al., 2019). Lung cancer is the largely widespread carcinogenesis in men and the third most familiar cancer in women. It is one of the largely aggressive human cancers that responsible for almost 1.4 million deaths per annum and has utmost mortality and incidence with 1.8 million new incidences and 1.6 million new deaths yearly (Moon et al., 2018). Lung cancer is characterized by four histological types of carcinoma such as adenocarcinoma, small cell, large cell and squamous cell carcinomas (Jiang et al., 2016).

Activation of apoptosis in cancer cell is one of the most important challenging about cancer treatment. Nowadays, researchers progressively more interested on the natural products for modifying apoptotic signaling (Zhang et al., 2014). Apoptosis controls tissue homeostasis in animals and it has two most important pathways: the mitochondrion or intrinsic arbitrated pathway and the death receptor or extrinsic arbitrated pathway, together of which outcome in the stimulation of diverse apoptotic proteins (Aas et al., 2015). The Bcl-2 family markers are critical controller in the activation of caspases and separated into pro-apoptotic (Bax) and anti-apoptotic (Bcl-2) proteins. Both of two apoptotic markers are associated with find out commitment or survival to apoptosis in cells (Gholami et al., 2013; Lindsay et al., 1813).

Development of lung cancer cell targeting drug along with none adverse effects to the normal cells is a difficult task in the area of cancer drug invention. The inadequate success of clinical therapies containing chemotherapy, surgery, radiation and immunomodulation in curing cancer, as evidenced by the increase mortality and morbidity rates, which also may generate severe side effects like leukopenia, bone marrow depression, alopecia and anaemia because of this indication there is a critical need of novel cancer management (Saravanakumar et al., 2014). Use of natural products and its derivatives for the growth of anticancer drugs are rising all over the world, for the reason that of smaller side effects as compared to synthetic drugs (Gupta et al., 2010). Medicinal plants has extensively exposed for reliable and excellent resources for the improvement of novel anti-cancer agents and exhibiting anti-proliferation, anti-inflammation, anti-metastatic and pro-apoptotic properties (Sun et al., 2009; Schwartsmann et al., 2002).

The metallic nanoparticles have gained a much attention in nowadays because of their their distinctive characteristics. In

recent years, a metallic oxide nanoparticles are examined broadly as an promising alternative agents in the field of biomedical science (Rahman et al., 2019; Umar et al., 2009; Rahman et al., 2017). The diverse synthesis procedures were executed to fabricate the metal oxide nanoparticles e.g. chemical, physical, and biological approaches. The synthesis of the metallic nanoparticles by green route method is regarded as an eco-friendly and inexpensive technique and demonstrated the various biological applications (Rahman et al., 2011; Rahman et al., 2017). The plants mediated bio-fabrication of the metal oxide nanoparticles is received the extensive interests in various fields. The metal oxide nanoparticles have extensive applications as an nano-medicine and diagnostics (Khan et al., 2011; Rahman et al., 2019; Rahman, 2011).

*Euphorbia fischeriana* (EF), a perennial herbaceous plant from Euphorbiaceae family and it is mostly dispersed on north China (Barrero et al., 2011). Recent studies reported the pure compounds and extracts of EF displayed a diversity of pharmacological activities, containing antimicrobial, antitumor, analgesic, immune enhancing, antiviral activities (Sun and Liu, 2011). Among them, the investigation associated to the anticancer properties has recently involved further interest. Extracts of EF have been confirmed to be successful towards various kinds of cancer, containing lung carcinoma, malignant melanoma and hepatocellular carcinoma in mice (Wang et al., 2010; Dong et al., 2016). For the best of our understanding, biological techniques of with plant extract of EF the first time as a reducing agent and surface stabilizing material for the ZnONPs formations. A lot of research had been confirmed on anticancer activities, but synthesis of nanoparticles specifically ZnONPs are insufficient. Therefore, in the current research, we have investigated the biological synthesis of ZnONPs by using the root of EF and notable these NPs by DLS, UV-vis spectroscopy, FTIR and TEM. Moreover, the synthesized EF-ZnONPs were determined for the anticancer and pro-apoptotic activity against A549 cells.

## 2. Materials and methods

### 2.1. Reagents and chemicals

MTT, DMEM, PBS, EtBr, DMSO and FBS were bought in Himedia-Lab Ltd., Mumbai, India. Zinc acetate dehydrates and DCFH-DA is attained from Sigma Aldrich (St. Louis, MO, USA). Entire other chemicals were utilized of diagnostic range. The primary antibodies for, Bax, Bcl-2, and  $\beta$ -actin were acquired in SantaCruzBiotechnology (SantaCruz, CA).

## 2.2. Cell culture

Lung cancer (A549) cells was sustained in DMEM with 10% of FBS and mixture antibiotics (streptomycin, penicillin and ampicillin 100 units/mL) under defined circumstances of temperature at 37°C, 95% humidity and 5% CO<sub>2</sub>. The cells obtain 80% of confluence were allowable to sub cultured using trypsin solution and employed for further work.

## 2.3. Preparation of EF root extraction

The root of EF was collected and rinsed with double distilled water. The root wa dried and powdered. The 2 g of EF root powder was heat macerated with the 100 ml of distied water at 60 °C for about 20 min. Afterward, the extract was chilled to 37 °C and sifted using filter paper and used for the synthesis of EF-ZnONPs.

## 2.4. Qualitative phytochemical analysis

The presence of main phytoconstituents like flavonoids, alkaloids, tannins, saponins, triterpenes, anthraquinones, sterols, polyphenols, coumarins, and proteins in the aqueous root extract of EF were investigated as per the procedures previously mentioned by the Harbone (Harbone, 1973; Harbone, 1973).

## 2.5. Synthesis of EF-ZnONPs

For the biosynthesis EF-ZnONPs, the quantity of 5 g zinc acetate dehydrate was combined with 50 ml of EF root extract at room temperature and at 90 °C under continuous stirring and studied the optimum time. ZnONPs were prepared after 72 h at room temperature and after 24 h at 90 °C.

## 2.6. Characterization of EF-ZnONPs

The characterization of synthesized EF-ZnONPs was proved by UV-Vis spectroscopy and spectral study was done in PerkinElmer Lambda-45 spectrophotometer at 200–700 nm. The morphology and size of synthesized EF-ZnONPs was exhibited via TEM analysis. The EF-ZnONPs for TEM were arranged through loading 10 µL of sample in a carbon painted copper grid and it was permitted to dehydrate for 15 min. FTIR spectral analysis was measured by working in transmission mode (500–4000 cm<sup>-1</sup>) for the EF-ZnONPs sample. The DLS was stated the size and size distribution of EF-ZnONPs.

## 2.7. Anticancer activity of EF-ZnONPs

### 2.7.1. Cell viability by MTT test

The cytotoxic properties of EF-ZnONPs were examined in A549 cells by MTT test explained previously (Leong et al., 2004). The A549 cells at  $2 \times 10^5$  cells/well were plated onto 96-wellplates. Then it was allowed to fix for 24 h previous to supplement and then added serial dosages (0–50 µg/ml) of EF-ZnONPs for 24 hrs. Later then, 5 mg/ml of MTT solution was added and incubated for 4 h (5% CO<sub>2</sub>) at 37°C. After that, MTT solutions were discarded and add DMSO in every well to

liquefy the formazan. Later than 10 min of incubation, the absorbance was taken at 570 nm.

### 2.7.2. Analysis of dual staining

Morphological alterations due to apoptosis were determined using AO/EtBr fluorescence staining (Ariffin et al., 2009). Two various concentrations of EF-ZnONPs (10 and 15 µg/ml) were selected for further analysis based on the MTT test. Cells were added with extracts for 24 hrs and treated with 10 µL of the reaction mixture (1:1 acridine orange-ethidium bromide). Later than 5 min of incubation, the cells were examined beneath the inverted microscope (Nikon Eclipse) at the 40× magnification.

### 2.7.3. Detection of intracellular ROS level

Intracellular ROS accretion was examined in A549 cells via the DCFH-DA staining technique (Jesudason et al., 2008). DCFH-DA is a fluorescent stain that can penetrate non-fluorescent probe that was utilized to measure the intracellular oxidant accretion status. Following treated with a range of doses (10 and 15 µg/ml) of EF-ZnONPs, 10 µM of DCFH-DA was added to cells and maintained for 30 min at 37 °C. Then cells were measured at emission/excitation wavelength of 485/535 nm in a microplate reader.

### 2.7.4. Determination of mitochondrial membrane potential (MMP)

MMP level was measured via Rh-123, lipophilic cationic stain (Johnson et al., 1980). A549 cells ( $1 \times 10^6$  cells/well) were loaded in 6-wellplate and supplemented with a range of doses (10 and 15 µg/ml) of formulated EF-ZnONPs. Later than 24hrs supplementation, cells were treated with Rh-123 for 30 min. Lastly, MMP was measured beneath the fluid cell imaging station at 485/530 nm in spectrofluorometer.

### 2.7.5. Cell migration assay

The A549 cells were cultured into 24-well. Later than 24 h maintenance at 37°C, cells were wounded by a 200 µl pipette tip to make a straight line. After 2 cleanse with PBS, different doses of EF-ZnONPs (10 and 15 µg/ml) was treated to a cells and then cells were incubated in a cell incubator in an environment including 5% CO<sub>2</sub> at 37°C for 36 h. The wound width was determined at four redefined locations when the wound was produced and after 0, 12, 24 and 36 h. The distances among the two edges of the wound were found at the reference points and statistically analyzed.

## 2.8. Western blotting analysis

A549 cells were added with EF-ZnONPs (10 and 15 µg/ml) for 24 h to investigate the expression of apoptotic markers. The protein quantification was completed as described earlier (Bhat et al., 2012). The 50 µgof proteins were resolved in 12% SDS-PAGE gels and translocated onto nitrocellulose membrane then blocked with fat less milk powder (5%). Moreover, it was developed with suitable primary antibodies (Santa Cruz Biotechnology, USA) likes Bax, Bcl-Xl and Bcl-2 (dilution of 1:1000) at 4°C overnight and secondary antibodies. The protein bands were observed by the ECL detection (Bio-rad, USA) method.

### 2.9. Statistical examination

Data was performed as mean  $\pm$  standard deviation (SD). The one-way ANOVA subsequently Duncan Multiple Range Test (DMRT) method was utilized to evaluate the means of various

groups by using SPSS 16 (SPSS, Inc., Chicago).  $P < 0.05$  was measured statistically relevant in all the groups.

## 3. Results

### 3.1. Result of preliminary phytochemical analysis of aqueous root extract of EF

The qualitative phytochemical analysis of the aqueous root extract of the EF was showed the existence of various phyto-constituents. Table 1 revealed the presence of alkaloids, flavonoids, saponins, triterpenes, anthraquinones, polyphenols, coumarins, and proteins in the aqueous root extract of EF.

### 3.2. Characterization of EF-ZnONPs

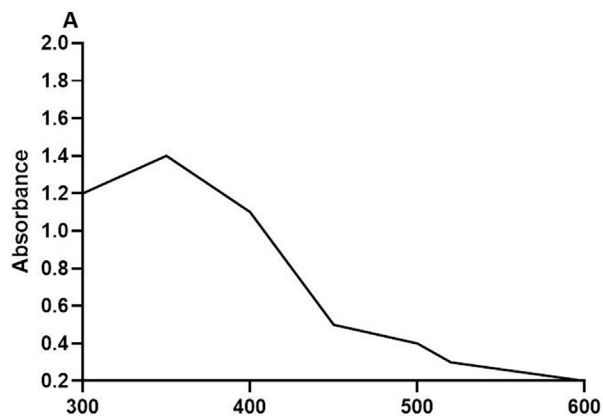
UV-vis spectroscopy is an imperative analytical method for categorization of NPs, which might suggest the evidence of ZnO synthesis due to distinctive absorption spectrum at 330 nm. It confirmed the formation of ZnONPs in the solution. The absorption spectrum of synthesized EF-ZnONPs is revealed in Fig. 1a.

TEM analysis demonstrated the core size of synthesized EF-ZnONPs to be 30 nm with a spherical morphology and

**Table 1** Result of qualitative phytochemical analysis of aqueous root extract of EF.

Phytochemicals	Aqueous extract
Alkaloids	+
Flavonoids	+
Saponins	-
Triterpenes	+
Tannins	-
Anthraquinones	+
Polyphenols	+
Sterols	-
Coumarins	-
Proteins	+

Note: '+'  $\rightarrow$  present '-'  $\rightarrow$  absent.



**B**

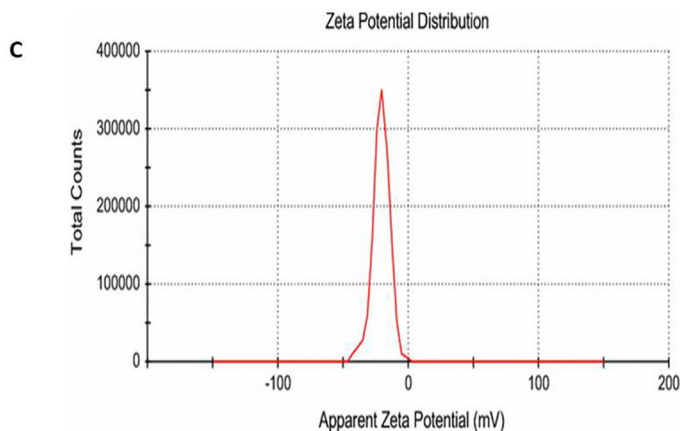
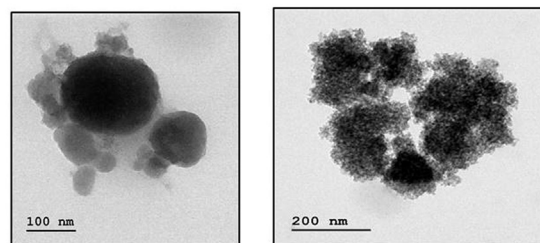


**Fig. 1** Characterization pattern of ZnONPs synthesised from EF. (a) UV-visible spectroscopic analysis of synthesized EF-ZnONPs. The distinctive absorption spectrum was noted at 330 nm, which proved the formation of EF-ZnONPs. (b) TEM analysis of synthesized EF-ZnONPs. TEM analysis demonstrated the core size of EF-ZnONPs to be 30 nm with a spherical morphology. (c) DLS analysis of synthesized EF-ZnONPs. DLS findings revealed a single-peak with a size of regarding 40 nm and a narrow distribution at 37 °C.

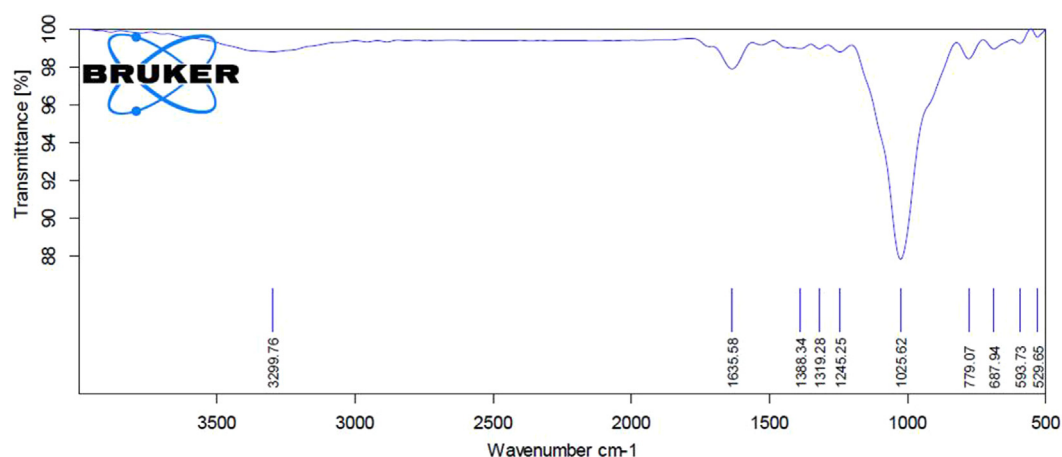


**Fig. 2** FTIR analysis of synthesized EF-ZnONPs. The FTIR measurements of the ZnONPs revealed numerous peaks that demonstrating the presence of diverse functional groups in the EF-ZnONPs.

proving the formation of zinc nanoparticles, which might have offered stabilization of synthesized nanoparticles (Fig. 1b).

The DLS was employed to observe the size and distribution diagram of EF-ZnONPs (Fig. 1c). DLS findings revealed a single-peak with a size of regarding 40 nm and a narrow distribution at room temperature.

The FTIR spectra studies were completed to verify the presence of various functional groups in the EF-ZnONPs (Fig. 2). The FTIR measurements of the ZnONPs revealed the presence of diverse functional groups, especially the peaks at  $3299.76\text{ cm}^{-1}$  (alkyne),  $1635.58\text{ cm}^{-1}$  (alkenes),  $1388.34\text{ cm}^{-1}$  (iso propyl group),  $1319.28\text{ cm}^{-1}$  (amines),  $1245.25\text{ cm}^{-1}$  and  $1025.62\text{ cm}^{-1}$  (esters),  $779.07\text{ cm}^{-1}$  and  $687.94\text{ cm}^{-1}$  (aromatic),  $593.73\text{ cm}^{-1}$  and  $529.65\text{ cm}^{-1}$  (halogen compound).

### 3.3. Anticancer activity of EF-ZnONPs

#### 3.3.1. Effect of EF-ZnONPs on MTT assay

To determine if EF-ZnONPs has antitumor effects in A549, an MTT test was employed to identify the viability of A549 cells following management with various doses (0 to  $50\text{ }\mu\text{g/ml}$ ) of EF-ZnONPs for 24 h. As represented in Fig. 3, A549 cell viability considerably lowered as the concentration of EF-ZnONPs augmented from 0 to  $50\text{ }\mu\text{g/ml}$ . The inhibitory concentration ( $\text{IC}_{50}$ ) point of the A549 cells was found as  $14.5\text{ }\mu\text{g/ml}$  and we have selected for 10 and  $15\text{ }\mu\text{g}$  concentrations of EF-ZnONPs for the further study.

#### 3.3.2. Effect of EF-ZnONPs on status of AO/EtBr

AO/EtBr dual staining was executed to find out the apoptotic cells (Fig. 4). The AO will stain the nuclei green through permeating into the cell membrane and EtBr will stain the nuclei red when the lost of cytoplasmic membrane integrity. The A549 cell treated the different concentrations (10 and  $15\text{ }\mu\text{g/ml}$ ) of EF-ZnONPs demonstrated more apoptotic cells than the control group.

#### 3.3.3. Effect of EF-ZnONPs on ROS production

The effectual of EF-ZnONPs on the accretion of ROS was observed by adding DCFH-DA that demonstrated improved fluorescent on production of intracellular oxidative stress

(Fig. 5). The A549 cells were treated with EF-ZnONPs resulting in significantly augments in the ROS generation in the dosages of 10 and  $15\text{ }\mu\text{g/ml}$  while comparing it to normal cells.

#### 3.3.4. Effect of EF-ZnONPs on the status of MMP

Due to electrophoretic accumulates in mitochondria, the control cells demonstrated elevated MMP with extreme green fluorescence, whereas supplemented with different range of EF-ZnONPs (10 and  $15\text{ }\mu\text{g/ml}$ ) treated A549 cells revealed reduced green fluorescence representing apoptotic cells (Fig. 6).

#### 3.3.5. Effect of EF-ZnONPs on cell migration assay

The A549 cells were supplemented with EF-ZnONPs and their cell migration potential was assessed by using a wound-healing test (Fig. 7). The cells were added various dosages of (10 and  $15\text{ }\mu\text{g/ml}$ ) EF-ZnONPs significantly inhibited the migration capability, whereas the control cells revealed increased cell proliferation.

### 3.4. Effect of EF-ZnONPs on apoptotic protein expression

The expressions of apoptotic proteins in control and EF-ZnONPs added A549 cells were exposed in Fig. 8. The normal cells demonstrated enhanced expression of Bcl-2 while, decreased expression o, Bax and Bid were found. EF-ZnONPs supplementation at various dosages (10 and  $15\text{ }\mu\text{g/ml}$ ) to A549 cells illustrated diminished expression of Bcl-2 and enhanced expressions of Bid and Bax were observed.

## 4. Discussion

Nanotechnology stands for an innovative and enabling proposal to generate new nanomaterials for a wide range of biomedical and biologic applications. Nanotechnology and nanoscience are paying attention a lot of interest due to the exciting and unique chemical and physical possessions of the nanomaterials (Zhao and Castranova, 2011; Wahid et al., 2019; Rahman et al., 2018; Umar et al., 2009). One of the most important applications of nanotechnology is its capability to

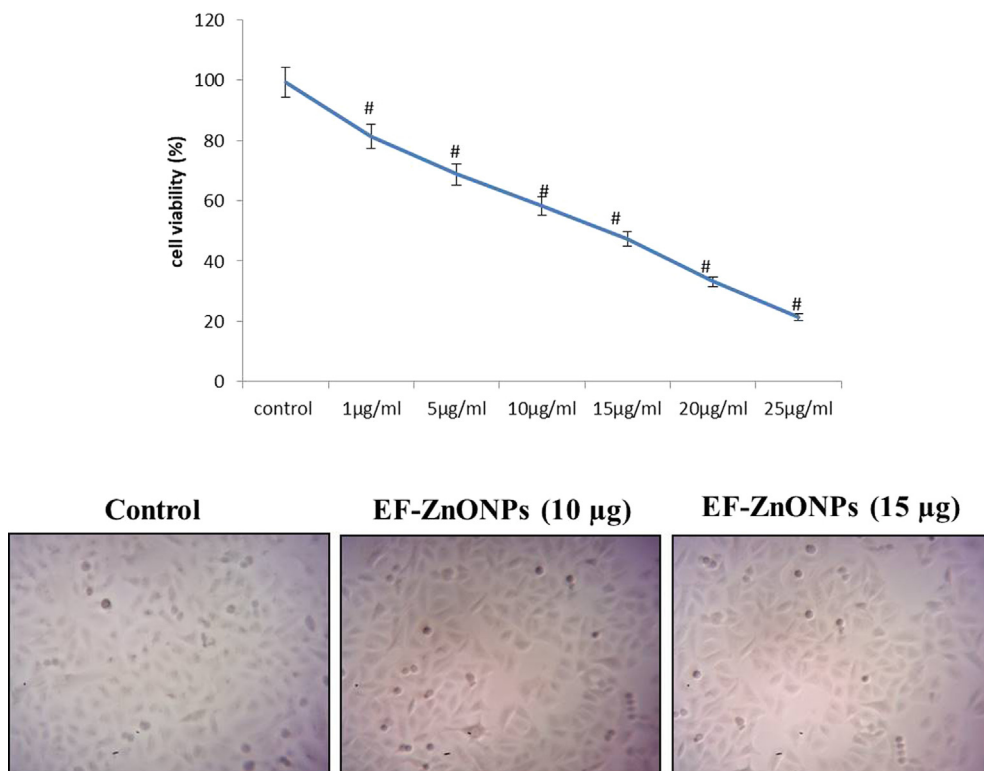


**Fig. 3** EF-ZnONPs inhibit the viability of A549 cells. The A549 cell viability considerably decreased as the concentration of EF-ZnONPs augmented from 0 to 50 µg/ml. The  $IC_{50}$  point of the A549 cells was found as 14.5 µg/ml and we have selected for 10 and 15 µg of EF-ZnONPs for the further study.

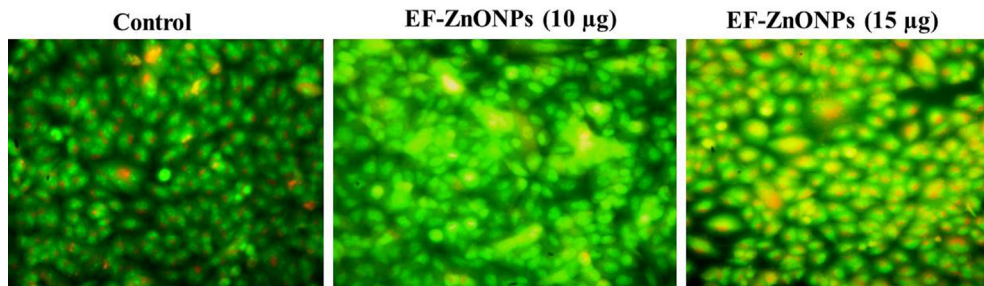


**Fig. 4** EF-ZnONPs activate apoptosis through activation of a dual staining method by AO/EtBr in A549 cells. The AO/EtBr stained A549 cell treated with the different concentrations of (10 and 15 µg/ml) EF-ZnONPs demonstrated more apoptotic cells than the control group.

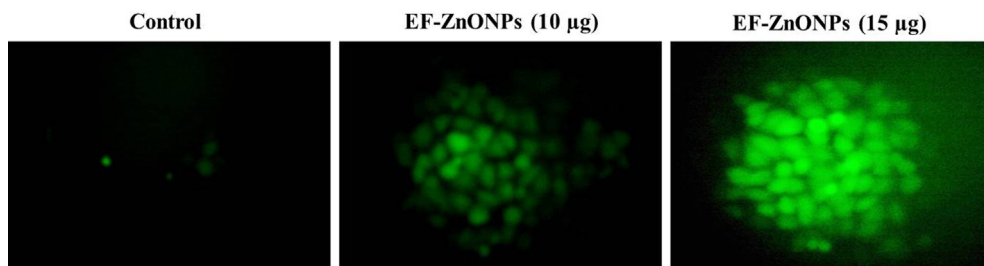


**Fig. 5** EF-ZnONPs stimulated intracellular ROS generation in A549 cells. The DCFH-DA staining of the A549 cells treated with EF-ZnONPs resulting in significantly augmented ROS production in the dosages of 10 and 15 µg/ml when compared to control cells.

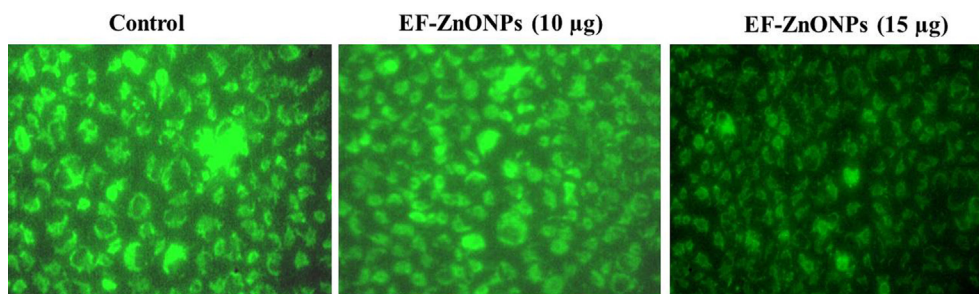


**Fig. 6** EF-ZnONPs decreased the MMP in A549 cells. The elevated MMP with extreme green fluorescence was noted at the control cells, whereas EF-ZnONPs (10 and 15 µg/ml) treated A549 cells revealed reduced green fluorescence representing the apoptotic cells.

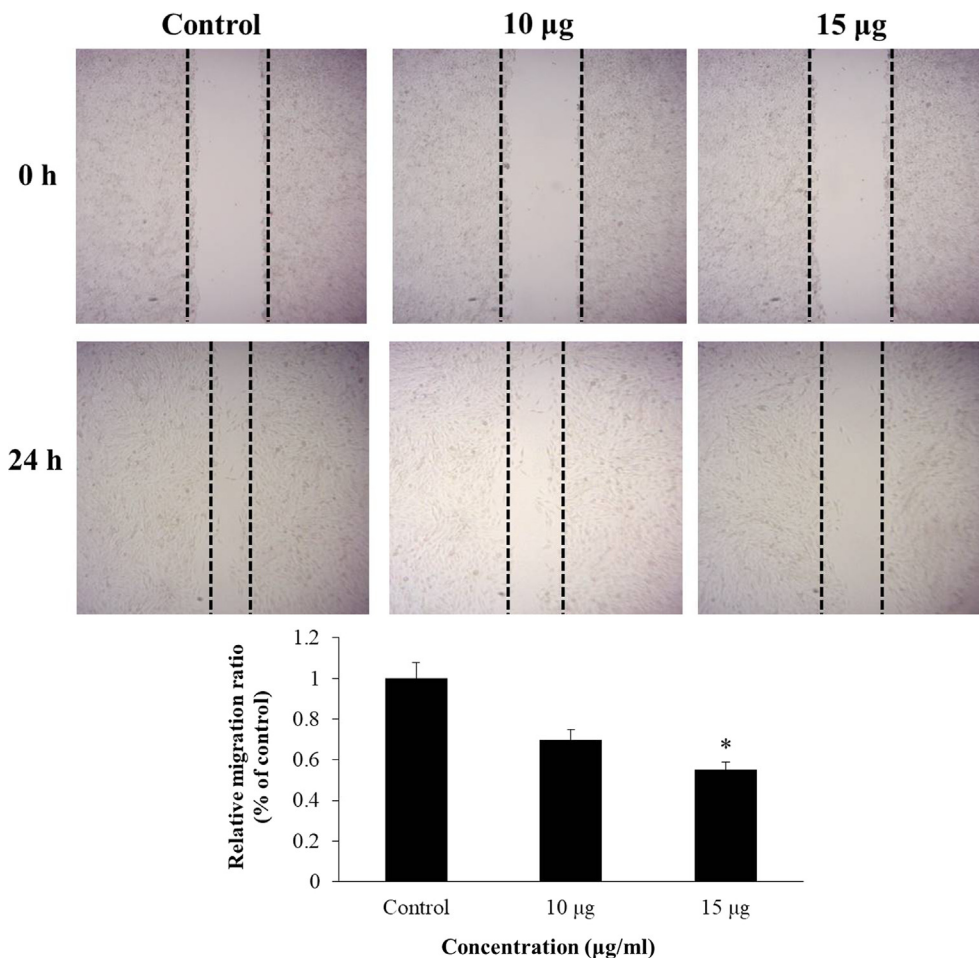


**Fig. 7** EF-ZnONPs inhibit the cell migration of A549 cells. The EF-ZnONPs (10 and 15 µg/ml) treated A549 cells significantly inhibited the cell migration, whereas the control cells revealed increased cell migration.

generate nanomaterials determining less than 100 nm in a controlled approach. Metal oxide in the nano range obtained distinctive activities that dependent on the size, surface chemistry and chemical composition (Umar et al., 2009; Umar et al., 2008). Metal oxide NPs like ZnONPs have been widely employed in cosmetic lotions, as these metals are identified to have effectual UV absorbing activities, thus acting as efficient UV blockers. Furthermore, recently, ZnONPs have been observing the possible for studied in cancer and biomedical purposes due to the attractive chemical activities (Baetke

et al., 2015). In this current work, prepared EF-ZnONPs were distinguished with FTIR spectroscopy, DLS, UV-visible and TEM observations. FTIR spectra demonstrated the presence of various bioactive compounds present in the formation of EF-ZnONPs. UV-visible spectroscopy finding demonstrated a sharp absorption in the wavelength were elucidated the basic band gap absorption of ZnO crystals. TEM examination revealed that ZnONPs had spherical morphology and that the average size of 30 nm, which was finally confirmed by DLS method.

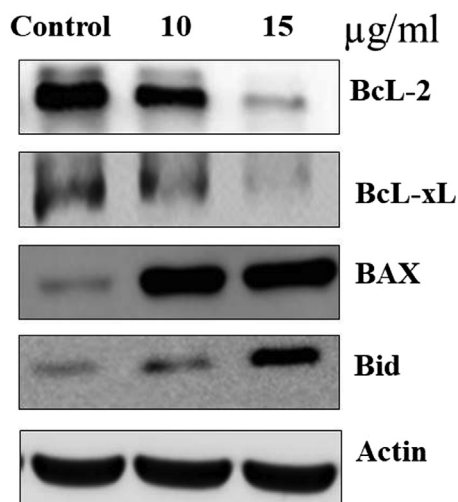


**Fig. 8** The anticancer effect of EF-ZnONPs on apoptosis signaling pathway protein expressions in A549 cells were analysed by western blotting. The EF-ZnONPs supplementation at various dosages (10 and 15  $\mu\text{g/ml}$ ) to A549 cells illustrated diminished expression of Bcl-2 and enhanced expressions of, Bax and Bid were observed.

The MTT test is a perfect technique for quantification of living cells, which can be differentiate the living and senescent or dead cells (Bai et al., 2017). In the current research, EF-ZnONPs treatments displayed cytotoxicity and inhibition of cell multiplication in A549 cancer cells in dose reliant approach is agreeing with earlier reports by *Euphorbia fischeriana* in B16 melanoma cells (Amaani and Dwira, 2018). Apoptosis is distinguished by morphological alterations like cell shrinkage, membrane blebbing, chromatin condensation and DNA degradation. It plays a main role in controlling growth, development and in the current approach, it has been an imperative goal for the improvement of efficiency anticancer drugs (Dong et al., 2016). Induction of apoptosis by the AO/EtBr stains, which confirm EF-ZnONPs treated cells exhibited chromatin condensation and nuclear fragmentation with yellow and orange nucleus revealing early and late apoptosis, whereas control cells were not observed these changes. These results were corroborated by previous studies by the *Croton bonplandianus* Baill. in A549 lung cancer cells (Nirmala et al., 2018).

ROS are either reactive anions or free radicals with peroxides and oxygen ions. Elevation of ROS can destroy the plasma membrane integrity and result in DNA break, progressively recognized as oxidative stress (Bhavana et al., 2016). Though, excess ROS status is risky to cells, the anticancer function of different treatments dependent on the capability to excite regulated ROS formation that modifies the cellular redox equilibrium directing to damage of mitochondria, oxidative stress and resulting induction of apoptosis (Simon et al., 2000). Several plant derivatives of natural drugs provoke the controlled formation of ROS, which activates cell death in different cancerous circumstances during apoptotic pathways (Engel and Evens, 2006). Our findings also supported this information through mitochondrial damage, by the augmented ROS formation and decreased MMP, which in turn controlled the apoptotic proteins expression during the treatment of EF-ZnONPs in A549 cells.

Apoptosis is a mainly general cell-death machineries, which play a very important function in the usual metabolic process. Tumor cells are differentiated via unrestrained development ranges and failure to apoptosis (Ismail et al., 2019). Stimulation of apoptosis is important for cell death mechanisms through anticancer mediators that destroys tumor cells. Agents that destroy or block cancer cell multiplication via activating apoptosis are recognized as hopeful antitumor agents (George and Abrahamse, 2019). Most phytochemicals stimulate apoptosis by the activation of the intrinsic apoptotic pathways that contains a variety of intracellular stimulus. A main arbitrators of this cascade contain pro (Bax) and anti (Bcl-2) apoptotic proteins (Omoyeni et al., 2015). Increased expression of Bax can induce apoptosis, whereas augmented Bcl-2 expression can reduce apoptosis (Kang and Reynolds, 2009). A variation in the range of those proteins results to damage of mitochondrial membrane and consequences in deliverance of cytochrome-c, which arbitrates the induction of caspase-9 (Zheng et al., 2016). Caspases are a most important class of proteases which participate a central function in cell death. Bax protein, an essential segment of mitochondrial-membrane, assists to transferring of cytochrome-c between the membranes, thus appearance of apoptotic remains and triggers caspase-9 and caspase-3 that ultimately lead to apoptosis (Fulda and Debatin, 2006; Julien and Wells, 2017). In the current study, EF-ZnONPs treatments activate the expression of Bax and Bid and suppressed the expression of Bcl-2 in A549 cells. Earlier studies also supported that the *Euphorbia fischeriana* triggered apoptosis in the cultured B16 melanoma cells (Wang et al., 2010).

## 5. Conclusion

In conclusion, we observed that the synthesized ZnONPs from EF was characterized by different techniques. It was primarily observed with the changes of color solution and UV absorption spectra also established the maximum absorbance peak. The TEM and DLS images exhibited the size and morphological structures of nanoparticles. The FTIR results illustrated synthesized EF-ZnONPs having various functional groups were observed. In addition, EF-ZnONPs induced cytotoxicity at a concentration range 14.5  $\mu\text{g/ml}$  and also activated apoptosis during increased ROS formation, decreased MMP, inhibited cell migration, altered AO/EtBr staining and induced pro-apoptotic and inhibited anti-apoptotic protein were observed.

## Funding

This project was supported by “the Fundamental Research Funds for the Central Universities” 1191320094.

## Declaration of Competing Interest

None of declares.

## References

- Aas, Z., Babaei, E., Hosseinpour Feizi, M.A., Dehghan, G., 2015. Anti-proliferative and apoptotic effects of dendrosomal farnesiferol C on gastric cancer cells. *Asian Pac J Can Prev* 16, 5325–5329.

- Amaani, R., Dwira, S., 2018. Phytochemical content an in vitro toxicity of Glycine soja ethanol extract on the A549 Lung cancer line cell. *J. PhyConf Ser.* 1073, 032042.
- Ariffin, S.H., Omar, W.H., Ariffin, Z.Z., Safian, M.F., Senafi, S., Wahab, R.M., 2009. Intrinsic anticarcinogenic effects of Piper sarmentosum ethanolic extract on a human hepatoma cell line. *Can. Cell Int.* 9, 6.
- Baetke, S.C., Lammers, T., Kiessling, F., 2015. Applications of nanoparticles for diagnosis and therapy of cancer. *Br. J. Radiol.* 88, 20150207.
- Bai, D.P., Zhang, X.F., Zhang, G.L., Huang, Y.F., Gurunathan, S., 2017. Zinc oxide nanoparticles induce apoptosis and autophagy in human ovarian cancer cells. *Int. J. Nanomed.* 12, 6521–6535.
- Barrero, R.A., Chapman, B., Yang, Y., Moolhuijzen, P., Keeble-Gagnère, G., Zhang, N., Tang, Q., Bellgard, M.I., Qiu, D., 2011. De novo assembly of Euphorbia fischeriana root transcriptome identifies prostratin pathway related genes. *BMC Genomics* 12, 600.
- Bhat, T.A., Nambiar, D., Pal, A., Agarwal, R., Singh, R.P., 2012. Fisetin inhibits various attributes of angiogenesis in vitro and in vivo—implications for angioprevention. *Carcinogenesis* 33, 385–393.
- Bhavana, J., Kalaivani, M.K., Sumathy, A., 2016. Cytotoxic and proapoptotic activities of leaf extract of Croton bonplandianus Baill. against lung cancer cell line A549, *Indian. J. Exp. Biol.* 54, 379–385.
- Dong, M.H., Zhang, Q., Wang, Y.Y., Zhou, B.S., Sun, Y.F., Fu, Q., 2016. Euphorbia fischeriana Steud inhibits malignant melanoma via modulation of the phosphoinositide-3-kinase/Akt signaling pathway. *ExpTher Med.* 11, 1475–1480.
- Dong, M.H., Zhang, Q., Wang, Y.Y., Zhou, B.S., Sun, Y.F., Fu, Q., 2016. Euphorbia fischeriana Steud inhibits malignant melanoma via modulation of the phosphoinositide-3-kinase/Akt signaling pathway. *ExpTher. Med.* 11, 1475–1480.
- Engel, R.H., Evens, A.M., 2006. Oxidative stress and apoptosis: a new treatment paradigm in cancer. *Front Biosci.* 11, 300–312.
- Fulda, S., Debatin, K.M., 2006. Extrinsic versus intrinsic apoptosis pathways in anticancer chemotherapy. *Oncogene* 25, 4798–4811.
- George, B.P., Abrahamse, H., 2019. Increased oxidative stress induced by rubus bioactive compounds induce apoptotic cell death in human breast cancer cells. *Oxid Med Cell Longev.* 2019, 6797921.
- Gholami, O., Jeddi-Tehrani, M., Iranshahi, M., Zarnani, A.H., Ziai, S. A., 2013. Umbelliprenin from ferulasowitsiana activates both intrinsic and extrinsic pathways of apoptosis in jurkat T-CLL cell line. *Iran J Pharm Res* 12, 371–376.
- Gupta, S.C., Kim, J.H., Prasad, S., Aggarwal, B.B., 2010. Regulation of survival, proliferation, invasion, angiogenesis, and metastasis of tumor cells through modulation of inflammatory pathways by nutraceuticals. *Can. Metastasis Rev.* 29, 405–434.
- Harbone, J., 1973. *Phytochemical Methods: A Guide to Modern Techniques of Plant Analysis.* Chapman & Hall, London.
- Ismail, N.I., Othman, I., Abas, F., Lajis, N.H., Naidu, R., 2019. Mechanism of apoptosis induced by curcumin in colorectal cancer. *Int J Mol Sci* 20, 2454.
- Jesudason, E.P., Masilamoni, J.G., Jebaraj, C.E., Paul, S.F., Jayakumar, R., 2008. Efficacy of DL-alpha lipoic acid against systemic inflammation-induced mice: antioxidant defense system. *Mol. Cell Biochem.* 313, 113–123.
- Jiang, Y., Zhang, L., Rupasinghe, H.V., 2016. The anticancer properties of phytochemical extracts from Salvia plants. *Botanics* 6, 25.
- Johnson, L.V., Walsh, M.L., Chen, L.B., 1980. Localization of mitochondria in living cells with rhodamine 123. *Proc. Natl. Acad. Sci USA* 77, 990–994.
- Julien, O., Wells, J.A., 2017. Caspases and their substrates. *Cell Death Differ.* 24, 1380–1389.
- Kang, M.H., Reynolds, C.P., 2009. Bcl-2 inhibitors: targeting mitochondrial apoptotic pathways in cancer therapy. *Clin. Can. Res.* 15, 1126–1132.
- Khan, S.B., Mohammed, M.F., Rahman, M., Jamal, A., 2011. Low-temperature growth of ZnO nanoparticles: photocatalyst and acetone sensor. *Talanta* 85, 943–949.
- Leong, C.O., Suggitt, M., Swaine, D.J., Bibby, M.C., Stevens, M.F., Bradshaw, T.D., 2004. *In vitro, in vivo,* and in silico analyses of the antitumor activity of 2-(4-amino-3-methylphenyl)-5-fluorobenzothiazoles. *Mol. Can. Ther.* 3, 1565–1575.
- Lindsay, J., Esposti, M.D., Gilmore, A.P., 1813. Bcl-2 proteins and mitochondria—specificity in membrane targeting for death. *BiochimBiophysActa* 2011, 532–539.
- Moon, J.Y., Manh Hung, L.V., Unno, T., Cho, S.K., 2018. Nobiletin enhances chemosensitivity to adriamycin through modulation of the Akt/GSK3 $\beta$ / $\beta$ catenin/MYC/MRP1 signaling pathway in A549 human non-small-cell lung. *Can Cells Nutr* 10, 1829.
- Nirmala, J.G., Celsia, S.E., Swaminathan, A., Narendhirakannan, R. T., Chatterjee, S., 2018. Cytotoxicity and apoptotic cell death induced by Vitisvinifera peel and seed extracts in A431 skin cancer cells. *Cytotechnology* 70, 537–554.
- Omoyeni, O.A., Hussein, A., Meyer, M., Green, I., Iwuoha, E., 2015. Pleiocarpapycnantha leaves and its triterpenes induce apoptotic cell death in Caco-2 cells in vitro. *BMC Complement Altern. Med.* 15, 224.
- Rahman, M.M., 2011. Fabrication of mediator-free glutamate sensors based on glutamate oxidase using smart micro-devices. *J. Biomed. Nanotechnol.* 7, 351.
- Rahman, M.M., Marwani, H.M., Agethami, F.K., Asiri, A.M., 2017. Xanthine sensor development based on ZnO-CNT, ZnO-CB, ZnO-GO and ZnO nanoparticles: an electrochemical approach. *New J. Chem.* 41, 6262–6271.
- Rahman, M.M., Alam, M.M., Asiri, A.M., Awual, M.R., 2017. Fabrication of 4-aminophenol sensor based on hydrothermally prepared ZnO/Yb<sub>2</sub>O<sub>3</sub> nanosheets. *New J. Chem.* 41, 9159–9169.
- Rahman, M.M., Alam, M.M., Asiri, M., 2018. Carbon black co-adsorbed ZnO nanocomposites for selective benzaldehyde sensor development by electrochemical approach for environmental safety. *J. Industrial Eng. Chem.* 65, 300–308.
- Rahman, M.M., Balkhoyor, H.B., Asiri, A.M., 2019. Removal of a melamine contaminant with Ag-doped ZnO nanocomposite materials. *New J Chem.* 43, 18848–18859.
- Rahman, M.M., Hussain, M.M., Asiri, A.M., 2019. D-Glucose sensor based on ZnO-V<sub>2</sub>O<sub>5</sub> NRs by an enzyme-free electrochemical approach. *RSC Adv.* 9, 31670–31682.
- Rahman, M., Jamal, A., Asiri, A.M., Abdullah, M.M., 2011. Synthesis, characterizations, photocatalytic and sensing studies of ZnO nanocapsules. *Appl. Sur. Sci.* 258, 672–677.
- Saravanakumar, T., Venkatasubramanian, P., Vasanthi, N.S., Manonmani Antimicrobial potential of Daruharidra (Berberis aristata DC) against the pathogens causing eye infection, *Int J Green Pharm.* 8 (2014).
- Schwartzmann, G., Ratain, M.J., Cragg, G.M., Wong, J.E., Saijo, N., Parkinson, D.R., Fujiwara, Y., Pazdur, R., Newman, D.J., Dagher, R., Di Leone, L., 2002. Anticancer drug discovery and development throughout the world. *J Clin Oncol.* 20, 47S–59S.
- Simon, H.U., Haj-Yehia, A., Levi-Schaffer, F., 2000. Role of reactive oxygen species (ROS) in apoptosis induction. *Apoptosis* 5, 415–418.
- Sun, Y.X., Liu, J.C., 2011. Chemical constituents and biological activities of Euphorbia fischeriana Steud. *Chem Biodivers.* 8, 1205–1214.
- Sun, Y., Xun, K., Wang, Y., Chen, X., 2009. A systematic review of the anticancer properties of berberine, a natural product from Chinese herbs. *Anticancer Drugs.* 20, 757–769.
- Umar, A., Rahman, M.M., Kim, S.H., Hahn, Y.B., 2008. Zinc oxide nanonail based sensor for hydrazine detection. *Chem. Comm.,* 166–169.
- Umar, A., Rahman, M.M., Al-Hajry, A., Hahn, Y.B., 2009. Highly-sensitive cholesterol biosensor based on well-crystallized flower-shaped ZnO nanostructures. *Talanta* 78 (1), 284–289.

- Umar, A., Rahman, M.M., Vaseem, M., Hahn, Y., 2009. Ultra-sensitive cholesterol biosensor based on low-temperature grown ZnO nanoparticles. *Electrochem Comm.* 11 (1), 118–121.
- Umar, A., Rahman, M.M., Hahn, Y.B., 2009. ZnO nanorods based hydrazine sensors. *J. Nanosci Nanotech.* 9 (8), 4686–4691.
- Wahid, A., Asiri, A.M., Rahman, M.M., 2019. One-step facile synthesis of Nd<sub>2</sub>O<sub>3</sub>/ZnO nanostructures for an efficient selective 2,4-dinitrophenol sensor probe. *Appl. Sur. Sci.* 487, 1253–1261.
- Wang, L., Duan, H., Wang, Y., Liu, K., Jiang, P., Qu, Z., Yagasaki, K., Zhang, G., 2010. Inhibitory effects of Lang-du extract on the in vitro and in vivo growth of melanoma cells and its molecular mechanisms of action. *Cytotechnology* 62, 357–366.
- Zhang, N., Wang, D., Zhu, Y., Wang, J., Lin, H., 2014. Inhibition effects of lamellarin D on human leukemia K562 cell proliferation and underlying mechanisms. *Asian Pac J Cancer Prev* 15, 9915–9919.
- Zhao, J., Castranova, V., 2011. Toxicology of nanomaterials used in nanomedicine. *J. Toxicol. Environ. Health B Crit. Rev.* 14, 593–632.
- Zheng, J.H., ViacavaFollis, A., Kriwacki, R.W., Moldoveanu, T., 2016. Discoveries and controversies in BCL-2 protein-mediated apoptosis. *FEBS J.* 283, 2690–2700.